INFLUENCE OF SEDIMENT TRANSPORT FORMULATION ON THE LINEAR STABILITY OF PLANAR AND BARRED COASTS

M.D. KLEIN

Section of Hydraulic Engineering, Faculty of Civil Engineering and Geosciences, Delft University of Technology, Stevinweg 1, P.O.Box 5048, 2600 GA Delft, The Netherlands

H.M. SCHUTTELAARS

Section of Hydraulic Engineering, Faculty of Civil Engineering and Geosciences, Delft University of Technology, Stevinweg 1, P.O.Box 5048, 2600 GA Delft, The Netherlands. Presently at Faculty of Geosciences, Utrecht University, The Netherlands.

M.J.F. STIVE

Section of Hydraulic Engineering, Faculty of Civil Engineering and Geosciences, Delft University of Technology, Stevinweg 1, P.O.Box 5048, 2600 GA Delft, The Netherlands

The linear stability of a planar and a barred coast is studied with a complex process-based model. By applying either the Engelund and Hansen or the Bailard sediment transport formulation, and a wave angle of approximately 5° in the breaker zone, the sensitivity of the linear stability characteristics to the sediment transport formulation is explored. Applying Engelund and Hansen to planar beaches, no fastest growing mode is found since the growth rate continuously increases with increasing wavelength. The corresponding bed perturbations are very oblique, down-current oriented bars. With Bailard, on the contrary, the growth rate increases with decreasing wavelength, suggesting that the preferred wavelength is somewhere between 0 and 300 m. The corresponding bed forms are up-current bars. Furthermore, the results show that inclusion of sediment transport in the direction of the wave orbital motion in both formulations is crucial for the growth of bed perturbations. When only (bed load) transport in the direction of the mean current is applied, stable up-current oriented bars are found. On barred beaches, both the Engelund and Hansen, and the Bailard formulation result in growing bed perturbations, consisting of rip channels around the crest of the breaker bar. Furthermore, in both cases fastest growing modes are found. The Bailard formulation results in a smaller longshore spacing of the rip channel system than the Engelund and Hansen formulation.

1. Introduction

Rhythmic coastal features are often observed in both the shoreline and the subtidal (barred) topography. They have been the subjects of many studies. Rhythmic shoreline features range from beach cusps of O(1 m) to coastline sand waves of O(1000 m), see, among others, Verhagen (1989) and Stive et al. (2002). Subtidal rhythmic features have length scales ranging from a few tens of meters to a few thousands of meters and consist mainly of rip channels and

crescentic patterns, see e.g. Bowen and Inman (1971), Wright and Short (1984), Konicki and Holman (2000) and Van Enckevort and Ruessink (2003).

One of the theories explaining surf zone rhythmicity is self-organization in the coupled hydro- and morphodynamic system, as introduced by Sonu (1968). The initial phase of self-organization can be studied with linear stability analysis (LSA). LSA's of both planar, e.g. Hino (1974), Christensen (1994), Falqués et al. (1996, 2000), Ribas et al. (2003) and Klein and Schuttelaars (2004), and barred beaches, e.g. Deigaard et al. (1999), Damgaard et al. (2002), Calvete et al. (2002), Klein et al. (2002) and Caballeria et al. (2003), have been performed before. The spreading in the results of these studies is large, both in the preferred spacing and in the shape of the bed perturbations. An important conclusion that can be drawn from these studies, however, is that the results are highly dependent on the applied sediment transport formulation.

In the present study, the effects of two sediment transport formulations on the stability properties of surf zone morphology are studied, viz. the Engelund and Hansen (1967) and the Bailard (1981) transport formula. Linear stability characteristics of a planar and a barred beach are studied by means of linear stability analysis using a process-based model. Using such model has two main advantages. First, the simplifications that are usually made in LSA's do not have to be made with this method. Second, any type of coast can easily be assessed. Furthermore, the linear analysis can easily be extended into the non-linear regime.

Both the water motion and the wave forces are calculated using a process-based, non-linear model. Due to the use of such model, the formal linearization that is usually made in LSA's can not be followed. Therefore another method of solving the linear stability problem has to be used, as discussed in Deigaard et al. (1999) and Klein et al. (2002).

This paper is organized as follows. First the model formulations and the method with which the linear stability characteristics are determined are discussed. Next, the results of the LSA of a planar beach are presented followed by the results of the LSA of a barred beach. Finally, the conclusions of this study are drawn.

2. Model description and Method

2.1. *Model Formulations*

The geometry that will be considered is that of an alongshore-uniform coast. The coastline is fixed, whereas the bed is erodible. Propagation, refraction and breaking of obliquely incident, short waves are computed with the HISWA wave

model (Holthuijsen et al., 1989), which is based on an evolution equation of the wave action density spectrum

$$\frac{\partial Nc_{g,x}}{\partial x} + \frac{\partial Nc_{g,y}}{\partial y} + \frac{\partial Nc_{g,\theta}}{\partial \theta} = -D_w \qquad (1)$$

in which x (y) is the cross-shore (longshore) coordinate, $N = E/\sigma$, where E [m^2/Hz] is the variance density and σ the wave frequency, $c_{g,x}$, $c_{g,y}$ [m/s] and $c_{g,\theta}$ [rad/s] the propagation speeds of wave action in the x, y and θ space. Furthermore, θ is the wave angle and D_w [m^2/s] the wave action dissipation, computed with the Battjes and Janssen (1978) formulations. Irregular waves with a significant wave height of 1.1 m and a peak period of 6 s are imposed as wave boundary conditions on the seaward, shore-parallel boundary of the model. The angle of wave incidence has been chosen such that the angle in the zone of breaking is approximately 5°. The water motion is described by the depth- and wave-averaged shallow water equations, consisting of the momentum equations

$$\frac{\partial u_c}{\partial t} + u_c \frac{\partial u_c}{\partial x} + v_c \frac{\partial u_c}{\partial y} + g \frac{\partial \eta}{\partial x} + \frac{\tau_x + F_x}{\rho_w D} - \nu \left(\frac{\partial^2 u_c}{\partial x^2} + \frac{\partial^2 u_c}{\partial y^2} \right) = 0 \qquad (2)$$

$$\frac{\partial v_c}{\partial t} + u_c \frac{\partial v_c}{\partial x} + v_c \frac{\partial v_c}{\partial y} + g \frac{\partial \eta}{\partial y} + \frac{\tau_y + F_y}{\rho_w D} - \nu \left(\frac{\partial^2 v_c}{\partial x^2} + \frac{\partial^2 v_c}{\partial y^2} \right) = 0 \qquad (3)$$

and the mass conservation equation

$$\frac{\partial \eta}{\partial t} + \frac{\partial u_c D}{\partial x} + \frac{\partial v_c D}{\partial y} = 0 \qquad (4)$$

In these equations, u_c (v_c) is the depth-averaged cross-shore (longshore) current velocity, t the time, g the gravitational acceleration, η the water level, τ_x and τ_y the bed shear stress components, ρ_w the water density, D the total water depth and ν the turbulent eddy viscosity. Furthermore, F_x and F_y are the wave force components per surface area, computed with the formulation of Dingemans et al. (1987), using the wave action dissipation. As flow boundary conditions, the longshore current velocities on the shore-perpendicular boundaries are prescribed. These velocities follow from the wave-driven longshore current. On the seaward, shore-parallel boundary a zero water level is prescribed. Note that the water motion is only forced by obliquely incident, breaking waves. Both the

effects of waves and currents are taken into account in the computation of the bed shear stresses, using a drag coefficient of 0.0035. The turbulent eddy viscosity is set to a uniform value of 1 m^2s^{-1}.

The bed evolves due to convergence and divergence of sediment fluxes. As mentioned before, two different sediment transport formulations are used, viz. the Engelund and Hansen (1967) and the Bailard (1981) formulation.

The Engelund and Hansen formulation for the total load, hereinafter designated as EH67, reads:

$$\vec{q} = \frac{0.05}{\sqrt{g}C^3(s-1)^2 D_{50}} \vec{u}^5 \tag{5}$$

in which C is the Chézy coefficient, s the relative density ρ_s/ρ_w with ρ_s the density of the sediment and D_{50} the median grain size.

The Bailard formulation for the suspended and bed load transport without bed slope effects, hereinafter designated as B81, reads:

$$\vec{q} = \frac{f_{cw}\varepsilon_b}{g(s-1)\tan\phi_i} \| \vec{u} \|^2 \vec{u} + \frac{f_{cw}\varepsilon_s}{g(s-1)w_s} \| \vec{u} \|^3 \vec{u} \tag{6}$$

in which f_{cw} is a friction factor accounting for waves and currents, ε_b (ε_s) the efficiency factor for bed (suspended) load, ϕ_i the angle of repose and w_s the sediment fall velocity. In order to account for the wave orbital velocity, $\vec{u}$ is defined as $\vec{u}_c + \vec{u}_0 \sin\phi t$ with $\vec{u}_c$ the mean velocity, $\vec{u}_0$ the rms wave orbital velocity vector and ϕ the peak frequency of the waves. In order to obtain the wave-averaged sediment transport rates, the procedure of Van der Molen (2002) has been followed.

2.2. Morphodynamic Equilibrium

Choosing an alongshore-uniform bottom profile, Eqs. 1 to 4 allow for a solution that is alongshore-uniform and time independent. From the mass conservation equation it follows that the cross-shore velocities are zero. Then Eqs. 2 and 3 reduce to

$$g\frac{\partial\eta}{\partial x} - \frac{F_x}{\rho_w D} = 0 \tag{7}$$

$$\frac{\tau_x}{\rho_w D} - \frac{F_x}{\rho_w D} - \nu\frac{\partial^2 v_c}{\partial x^2} = 0 \tag{8}$$

In cross-shore direction the wave forcing is balanced by the pressure term, resulting in an alongshore-uniform wave set-up. In longshore direction, the bed

shear stress, wave forcing and mixing term balance each other, driving an alongshore-uniform current.

Because of the contribution of sediment transport in the direction of the wave orbital motion, the alongshore-uniform bottom applied in the complex model is no equilibrium bottom in the strictest sense. However, it has been verified that the bed changes due to the divergences and convergences of the sediment transport associated with the alongshore-uniform beach are negligible compared to those resulting from the rhythmic coastal features studied in this paper. This result confirms the validity of the implicit assumption often made in linear stability analyses that the 2DV morphological development of coastal systems is typically slower than the 2DH or 3D morphology, which is studied in this paper. This assumption is also validated by observations, see Ruessink et al. (2000) and Plant et al. (2001).

2.3. *Linear Stability Analysis*

The system of equations allows for a morphological equilibrium solution $\Phi = \Phi_{eq}$, with $\Phi = \Phi(u,v,D)$. It is not clear whether or not this morphological equilibrium is stable. Therefore a LSA is performed. This means that the solution $\Phi = \Phi_{eq} + \Phi'$ is substituted in the equations with a perturbation Φ' much smaller than Φ_{eq}. Next, the system of equations is linearized with respect to the perturbations. This results in an eigenvalue problem. Focussing on the bed perturbations, it can be shown that the solution has the form

$$h' = A_i(x)\exp[iky - i\omega t] \tag{9}$$

in which h' is the bed perturbation, $A_i(x)$ the complex cross-shore amplitude function (eigenfunction), k the alongshore wave number, ω the complex angular frequency (eigenvalue) and i the imaginary unit. The imaginary part (ω_i) of the complex eigenvalue represents the growth rate of the perturbation and the real part (ω_r) the alongshore migration of the perturbation.

In this study, the water motion corresponding to a perturbed topography (the bed perturbation is constructed by an amplitude function and a wavelength that can be freely chosen) is calculated with a fully non-linear, process-based model. Therefore, a formal linearization can not be performed. In order to mimic the linear system, the amplitude of the perturbation is chosen sufficiently small, hence non-linear terms are negligible in the equations. In practice this is realized by choosing the amplitude of the perturbation not larger than 1 % of the water depth. An iteration process is used to find the solution (i.e. bed perturbation and

corresponding eigenvalue) with the largest positive real part of the eigenvalue, i.e. the solution that initially grows fastest.

In order to start the iteration process, we need to make a first estimate of the cross-shore amplitude function of the perturbation. It was verified that the final solution is independent of the initially chosen cross-shore amplitude distribution. During every iteration the bed perturbation is derived from a Fourier analysis, retrieving the cross-shore amplitude function A_i, which only contains the changes of the perturbation related to the wave number k. This amplitude distribution is rescaled such that the amplitude is again smaller than 1 % of the local water depth. Based on the cross-shore amplitude function $A_{i-1}(x)$ at the start of the iteration and the newly computed one $A_i(x)$, the Rayleigh quotient R (Griffel, 1985) is obtained:

$$R = -i\omega = \frac{\int_0^\infty A_{i-1}^*(x)A_i(x)dx}{\int_0^\infty A_{i-1}^*(x)A_{i-1}(x)dx} \tag{10}$$

in which * denotes the complex conjugate. This Rayleigh quotient is an estimate for the eigenvalue corresponding to the largest growth rate. Since the iteration process starts with an estimate for the eigenfunction, it is likely that after one iteration both $A_i(x)$ and ω are polluted with other modes than the one with the largest growth rate. After every iteration, $A_i(x)$ and ω are better estimates of the solution corresponding to the largest growth rate. Constructing a new perturbation for every iteration, based on the results of the previous iteration, the eigenvalues found will converge towards the eigenvalue with the largest growth rate. The accuracy criterion for convergence has been set to 0.5 %. If both the real and the imaginary part of the eigenvalue change less than 0.5 % with respect to those previously computed, the iteration process is assumed to have converged. In that case, $A_i(x)$ is the eigenfunction, describing the spatial structure of the fastest growing mode and the Rayleigh quotient R is the eigenvalue.

Note that only one alongshore wavelength is considered and that the eigenfunction with the largest growth rate associated to that wavelength is found. Applying this method to a range of wavelengths yields the growth rate as a function of the alongshore wavelength. If for a certain wavelength the growth rate is maximal, the bed perturbation corresponding to this wavelength λ_p is designated as the fastest growing mode (FGM).

3. Numerical Results: Planar Beach

In this section the results of LSA's of a planar sloping beach with a slope of 0.0075 are discussed. A much more elaborated study on the linear stability of planar beaches can be found in Klein and Schuttelaars (2004).

The growth rates as a function of the alongshore wavelength, obtained with EH67 and B81, are depicted in Figure 1. Although the growth rates are positive, and hence the coastal system is unstable, no FGM has been found in the considered wavelength range. In case of EH67, the growth rate increases with increasing wavelength, whereas in case of B81 the growth rate decreases with increasing wavelength. These results suggest that in case of EH67 in the limit of $\lambda \rightarrow \infty$ the growth rate goes to a limit value, which is finite and positive.
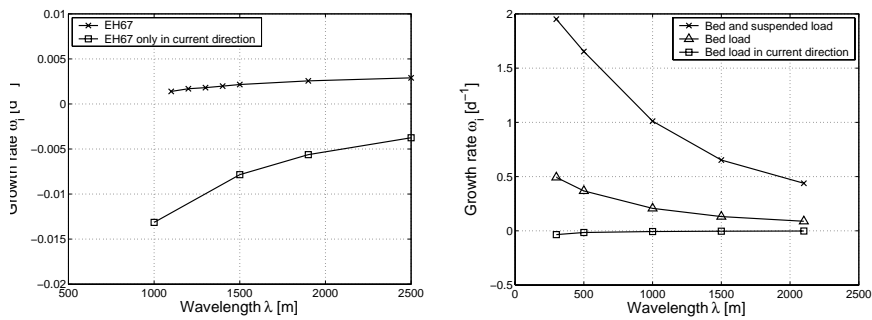
Figure 1. Growth rate vs. wavelength obtained with EH67 (left) and with B81 (right) in case of a planar sloping beach.

In case of B81, no FGM has been found in the considered wavelength range. It is likely that a FGM exists, but the spacing is smaller than the minimum wavelength of 300 m that can be assessed with the present model set-up. Adding bed slope effects should cause a shift of the preferred spacing towards larger wavelengths since the bed slope effects are stronger for small wavelengths than for large wavelengths. Including bed slope effects is left for further study.

Note that besides the qualitative differences in the growth rates, also the magnitude of the growth rates are different. B81 results in growth rates that are much larger than the ones obtained with EH67.

Furthermore, the influence of the different transport modes in the EH67 and B81 formulations has been investigated. The right panel of Figure 1 demonstrates that omitting the suspended sediment transport from the B81 formulation does not change the qualitative dependence of the growth rate on the wavelength, although the growth rates are significantly smaller.

The results of both EH67 and B81 change dramatically when omitting the (bed load) transport in the direction of the wave orbital motion. In that case the growth rate becomes negative and increases with increasing wavelength, suggesting that for $\lambda \rightarrow \infty$ the growth rate goes to zero.

Despite the large differences in the growth rates obtained with the two transport formulas, the migration celerities are of the same order of magnitude

for both sediment transport formulations, viz. a few tens of meters per day (the migration celerity is not displayed in a figure).
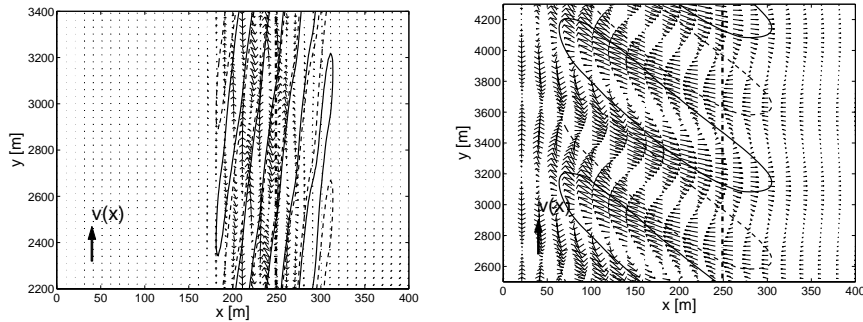

Figure 2. Characteristic bed and flow perturbations obtained with EH67 (left) and with B81 (right) in case of a planar sloping beach. The dash-dotted line indicates the breaker line, defined as the cross-shore location where maximum wave energy dissipation occurs. Coastline is at x=0.

Two characteristic bed and flow perturbations obtained with EH67 and B81 are depicted in Figure 2. The direction of the mean longshore current is indicated, as well as the breaker line, defined as the cross-shore location where maximum wave energy dissipation occurs. The bed perturbations obtained with EH67 are very oblique down-current oriented bars with onshore flow over the shoals (solid contours) and offshore flow over the troughs (broken contours). The orientation is with respect to the (virtual) point of shore attachment. Other experiments of this series showed that the obliqueness increases with increasing wavelength, and thus with increasing growth rate. The perturbed flow pattern changes from a circulation pattern for small wavelengths into a pattern with no cross-shore velocities for large wavelengths. These results suggest that the orientation of the bed forms becomes shore-parallel for $\lambda \to \infty$. Omitting the sediment transport in the direction of the wave orbital velocity from EH67 yields up-current oriented bars for an angle of 5°. The dependence of the bar orientation on the angle of wave incidence when omitting the sediment transport in the direction of the wave orbital velocity has not been investigated.

In case of B81, on the contrary, up-current oriented bars are found. This is true for the three transport modes that have been considered, viz. the complete B81 formulations, only bed load transport and bed load transport only in the direction of the wave orbital motion. It has to be remarked that this applies only to wave angles at the 'breaker line' smaller than approximately 7°. For larger wave angles, the results of the LSA obtained with B81 become very similar to the results of the LSA obtained with EH67, viz. very oblique down-current

oriented bars with the growth rate increasing with increasing wavelength. See Klein and Schuttelaars (2004) for more details.
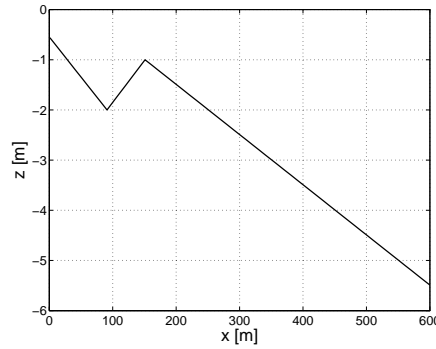
4. Numerical Results: Barred Beach

Figure 3. The alongshore-uniform single-barred coastal profile.

This section discusses the results of LSA's of a barred coast performed with EH67 and B81. The coastal profile that has been used is displayed in Figure 3. Note that the water depth at $x = 0$ is not equal to zero. The same wave forcing ($H_s = 1.1$ m and a wave angle of 5° at the bar crest) as applied to planar beaches has been applied in the LSA of single-barred beaches.
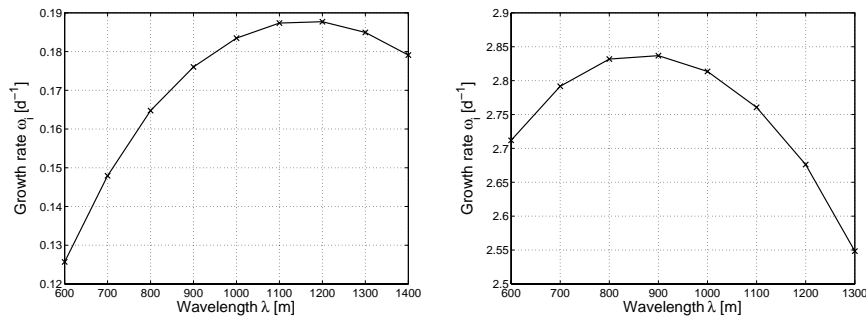

Figure 4. Growth rate vs. wavelength obtained with EH67 (left) and with B81 (right) in case of a single-barred beach.

The growth rate as a function of the alongshore wavelength obtained with the two different sediment transport formulations are depicted in Figure 4. It is clear that for both series of experiments a FGM exists, although with different preferred wavelengths. In case of EH67 the preferred wavelength is 1200 m, whereas in case of B81 the preferred wavelength is 900 m. Furthermore, the growth rates obtained with B81 are an order of magnitude higher than the ones obtained with EH67. However, these differences in the magnitude of the growth

rates are not as large as the differences between the growth rates obtained for planar beaches. The migration celerities of the FGM's are 168.6 and 135.3 md^{-1} for EH67 and B81, respectively, which compare well with observations.

The bed and flow perturbations corresponding to the two FGM's are depicted in Figure 5. The direction of the mean longshore current is indicated, as well as the crest of the breaker bar. The bed perturbations obtained with the two sediment transport formulations do not essential differ from each other. They can be characterized as rip channel systems with alternating shoals (solid contours) and troughs (dashed contours) around the crest of the breaker bar. The perturbed flow patterns do not essentially differ from each other and consist of circulation cells with onshore flow over a shoal in the breaker zone and offshore flow over a channel in the breaker zone.
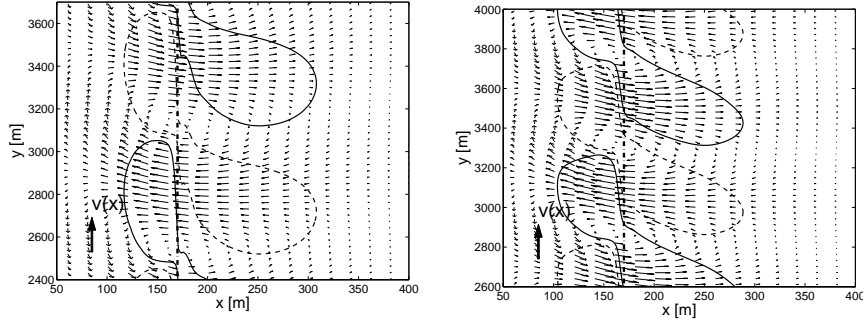

Figure 5. Bed and flow perturbations of the FGM's obtained with EH67 (left) and with B81 (right) in case of a single-barred beach. The dash-dotted line indicates the crest of the breaker bar.

5. Discussion

The mechanism explaining the growth of bed perturbations has been introduced in Falqués et al. (1996) and has been elaborated further by Ribas et al. (2003) and Klein and Schuttelaars (2004). The mechanism is based on the cross-shore gradient of the ratio of the wave stirring function and the equilibrium depth. This ratio is designated as the potential stirring function. All sediment transport formulations can be written in a form $\vec{q} = \alpha(x)\vec{u}$ in which $\alpha(x)$ is the wave stirring function. Note that in case of EH67 this wave stirring function is proportional to $\vec{u}^4$ and in case of B81 proportional to $\vec{u}^2$.

The present study shows that on planar beaches this wave stirring function is crucial for the shape of the bed perturbation, the sign and the magnitude of the growth rate, see also Ribas et al. (2003) and Klein and Schuttelaars (2004). Although the wave stirring in case of B81 is indeed larger than in case of EH67, it can not be completely held responsible for the large difference (two orders of magnitude) in the magnitude of the growth rates obtained with EH67 and B81.

This is confirmed by LSA's with B81 and wave angles larger than 7°, in which the same down-current oriented bars with similar growth rates as EH67 are found. From this must be concluded that not only the wave stirring function but also the orientation of the bars determine the growth rate. Due to the obliqueness of the down-current oriented bars, the gradients in the sediment transport rates, and hence the growth rates, are small, much smaller than the gradients in the sediment transport rates associated with the less oblique, up-current oriented bars obtained with B81 and with relatively small angle of wave incidence.

The present study also shows that for barred coasts, the shape of the wave stirring is not crucial for an unstable coast to occur, since the cross-shore gradient of the potential stirring function is dominated by the topography. The spatial structures and the migration rates of bed perturbations on barred beaches obtained with the two sediment transport formulations are much more similar than they are on planar beaches. The difference between the growth rates has decreased to one order of magnitude. Since the spatial structures obtained with EH67 and B81 are similar and the equilibrium profile is identical, this difference must be caused by the wave stirring function.

Figure 3 shows that the applied barred profile is schematized to a large extent. In order to assess the effects of this schematization, an experiment with a smooth cross-shore profile has been performed, giving similar results. This, however, only applies to sufficiently mild slopes (less than 1:50) of the seaward side of the breaker bar.

6. Conclusions

In this paper the linear stability characteristics of a planar and a barred beach are studied using a process-based model. The focus is on the influence of the sediment transport formulation. Therefore both the Engelund and Hansen (1967) and the Bailard (1981) formulation for sediment transport have been used. From the results of the LSA it is apparent that the effects of the sediment transport formulation on the linear stability characteristics of planar beaches are very large. First of all, the orientation of the bed perturbations is different. In case of EH67 down-current bars are found, which become more oblique with increasing wavelength. With B81, on the contrary, up-current oriented bars are found, as long as the angle of wave incidence at the breaker line is smaller than 7°. With EH67 no FGM exists since the growth rate increases with increasing wavelength without reaching a maximum. In case of B81 FGM's are likely to exist but the preferred spacing is smaller than the minimum spacing of 300 m that can be assessed with the present model set-up.

From the results of LSA's of planar beaches it is apparent that for both EH67 and B81 the contribution of the sediment transport in the direction of the wave orbital motion is essential for positive growth rates, and hence for growing morphological features.

The influence of the sediment transport formulation on the results of LSA's of single-barred beaches is more limited. For both EH67 and B81 fastest growing modes are found with spatial structures that are rather similar, viz. a rip channel system with alternating channels and shoals around the crest of the breaker bar. The different sediment transport formulations do, however, result in different spacings and growth rates. The EH67 generally results in bed perturbations with larger spacings and with smaller growth rates.

Acknowledgements

References

Bailard, J.A. (1981). An energetics total load sediment transport model for a plane sloping beach. *J. Geophys. Res., 86 (C11),* pp. 10983-10954.

Battjes, J.A. and Janssen, J.P.F.M. (1978). Energy loss and set-up due to breaking in random waves. *Proc. 16th Int. Conf. Coastal Eng.*, pp. 569-587.

Bowen, A.J. and Inman, D.L. (1971). Edge waves and crescentic bars. *J. Geophys. Res., 83,* pp. 8662-8671.

Caballeria, M., Coco, G. and Falqués, A. (2003). Crescentic patterns and self-organization processes on barred beaches. *Proc. Int. Conf. Coastal Sediments,* cd-rom published by World Scientific Publishing Corp. and East Meets West Productions, ISBN 981-238-422-7.

Calvete, D., Dodd, N. and Falqués, A. (2002). Morphological development of nearshore bed forms. Falqués, A., Montoto, A. and Iranzo, V. (1996). Coastal morphodynamic instabilities. *Proc. 28th Int. Conf. Coastal Eng.*, pp. 3321-3332.

Christensen, E.D., Deigaard, R. and Fredsøe, J. (1994). Sea bed stability on a long straight coast. *Proc. 24th Int. Conf. Coastal Eng.*, 1865-1879.

Damgaard, J., Dodd, N., Hall, L. and Chesher, T. (2002). Morphodynamic modelling of rip channel growth. *Coastal Engineering, 45,* pp. 199-221.

Deigaard, R. and Drønen, N., Fredsøe, J., Jensen, J.H. and Jørgensen, M.P. (1999). A morphological stability analysis for a long straight barred coast. *Coastal Engineering,* 36, 171-195.

Dingemans, M.W., Radder, A.C. and De Vriend, H.J. (1987). Computations of driving forces of wave-induced currents. *Coastal Engineering, 11,* pp.539-563.

Engelund, F. and Hansen, E. (1967). *A monograph on sediment transport in alluvial streams.* Technisk Forlag, Copenhagen, Denmark.

Falqués, A., Montoto, A. and Iranzo, V. (1996). Bed-flow instabilities of the longshore current. *Continental Shelf Research*, pp. 1927-1964.

Falqués, A., Coco, G. and Huntley, D.A. (2000). A mechanism for the generation of wave-driven rhythmic patterns in the surf zone. *J. Geophys. Res., 105(C10),* pp. 24071-24087.

Hino, M. (1974). Theory on the formation of rip-current and cuspidal coast. *Proc. 14th Int. Conf. Coastal Eng.*, pp. 901-919.

Klein, M.D. and Schuttelaars, H.M. (2004). Importance of sediment transport in direction of the wave orbital velocity for the linear stability of planar beaches. *Submitted to J. Geophys. Res.*

Klein, M.D., Schuttelaars, H.M. and Stive, M.J.F. (2002). Linear stability of a double-barred beach. *Proc. 28th Int. Conf. Coastal Eng.*, pp. 3396-3408.

Konicki, K.M. and Holman, R.A. (2000). The statistics and kinematics of transverse sand bars on an open coast. *Marine Geology, 169,* pp. 69-101.

Plant, N.G., Ruessink, B.G. and Wijnberg, K.M. (2001). Morphological properties derived from a simple cross-shore sediment transport model. *J. Geophys. Res., 106(C1),* pp. 945-958.

Ribas, F., Falqués, A. and Montoto, A. (2003). Nearshore oblique sand bars. *J. Geophys. Res.,108(C4),* 3119, doi:10.1029/2001JC000985.

Ruessink, B.G., van Enckevort, I.M.J., Kingston, K.S. and Davidson, M.A. (2000). Analysis of observed two- and three-dimensional nearshore bar behaviour. *Marine Geology, 169,* pp. 161-183.

Sonu, C.J. (1968). Collective movement of sediment in littoral environment *Proc. 11th Int. Conf. Coastal Eng.*, pp. 373-400.

Stive, M.J.F., Aarninkhof, S.G.J., Hamm, L.H.H., Larson, M., Wijnberg, K.M., Nicholls, R.J. and Capobianco, M. (2002). Variability of shore and shoreline evolution. *Coastal Engineering, 47,* pp. 211-235.

Van der Molen, J. (2002). The influence of tides, wind and waves on the net sand transport in the North Sea. *Continental Shelf Research, 22,* pp. 2739-2762.

Van Enckevort, I.M.J. and Ruessink, B.G. (2003). Video observations of nearshore bar behaviour. Part 2: alongshore non-uniform variability. *Continental Shelf Research, 23,* pp. 513-532.

Verhagen, H.J. (1989). Sand waves along the Dutch coast. *Coastal Engineering, 13*, pp. 129-147.

Wright, L.D. and Short, A.D. (1984). Morphodynamic variability of surf zones and beaches: a synthesis. *Marine Geology, 56,* pp. 93-118.